International Journal of Heat and Fluid Flow 29 (2008) 1456–1461

Contents lists available at ScienceDirect

International Journal of Heat and Fluid Flow

journal homepage: www.elsevier.com/locate/ijhff

Thermal conductivity measurement and sedimentation detection of aluminum oxide nanofluids by using the 3ω method

Dong-Wook Oh [a], Ankur Jain [b], John K. Eaton [c], Kenneth E. Goodson [c], Joon Sik Lee [a,*]

[a] School of Mechanical and Aerospace Engineering, Seoul National University, Seoul 151-744, Republic of Korea
[b] Silicon Technology Solutions, Freescale Semiconductor, Austin, TX 78754, USA
[c] Department of Mechanical Engineering, Stanford University, Stanford, CA 94305, USA

ARTICLE INFO

Article history:
Received 20 November 2007
Received in revised form 16 April 2008
Accepted 17 April 2008
Available online 10 June 2008

Keywords:
3ω method
Al_2O_3 nanoparticle
Thermal conductivity
Nanofluid
Sedimentation

ABSTRACT

Suspensions of nano-sized solid particles in a liquid medium, known as nanofluids show remarkable enhancement in thermal conductivity compared to the base fluid. Nanofluids are a promising candidate for advanced heat transfer applications such as microelectronics cooling. While the thermal conductivity of nanofluids has been measured in the past using conventional techniques such as the transient hot wire method, this work presents the application of the 3-omega (3ω) method for this purpose. The theoretical model for 3ω response of a heater device with de-ionized (DI) water and ethylene glycol (EG) is verified by comparing with experimental measurements. Following this validation, the effective thermal conductivity of Al_2O_3 nanofluids in DI water and EG are measured at room temperature. In addition, interesting effects in the thermal response due to agglomeration and sedimentation of nanoparticles are observed.

1. Introduction

Nanofluid is a suspension of nanoscale particles such as metal, metal oxide or carbon nanotube (CNT) in the base fluids such as water and ethylene glycol (EG). The nanofluids have drawn much attention in the heat transfer society since the finding of Masuda et al. (1993) that the increment of the effective thermal conductivity of nanofluids exceeds the estimates by conventional theories such as the effective medium approximation by Maxwell (1892) and the Hamilton–Crosser model(1962). With only a small volume fraction of nanoparticles, generally less than 5%, the reported effective thermal conductivities of the nanofluids vary from a few percent increment to even a couple of folds (Wang and Mujumdar, 2007) compared with those of the pure base fluids. Large potential economic benefit of the nanofluid technology for increasing efficiency of heat exchangers is anticipated since more than $ 80 billion dollars annually are spent on energy for air conditioning and refrigeration equipment, in the United States alone (Marquis and Chibante, 2005).

However, as pointed out by Kabelac and Kuhnke (2006), different research groups reported widely spreaded experimental values of nanofluid conduction as well as convection heat transfer because the thermophysics and electrochemistry of nanoscale particle–particle and particle–medium interactions are not fully understood. The aggregation of nanoparticles and the resulting time dependence of the nanofluid on the thermal conductivity may be one of the reasons for the discrepancies in the literature (Hong et al., 2006; Prasher et al., 2006). The aggregated nanoparticles in suspension are hard to break even with intensive ultrasonic vibrations. As a result, sedimentation occurs which leads to non-homogenous nanoparticle dispersions and possible fouling. The colloidal instability is also one of the biggest problems that make the commercial use of nanofluids difficult.

Most of the nanofluid thermal conductivity measurements reported in the literature have been conducted by using the transient hot wire method (THW). In this method, a vertical hot wire is placed inside a nanofluid-filled cylinder. DC or AC heat generation is applied to the hot wire, and the temperature change with time is measured to calculate the nanofluid thermal conductivity (Lee et al., 1999). Das et al. (2003) used the temperature oscillation method to measure the thermal conductivity of nanofluids. These methods measure the temperature response of the nanofluid when temperature oscillation or heat flux is imposed. The measured temperature response of the nanofluid is the result of averaged or localized thermal conductivity in the direction of nanofluid chamber height. The data can be misleading if sedimentation of agglomerate nanoparticle occurs since, in such a case, the thermal conductivity of the nanofluid becomes a function of the fluid chamber height.

In this paper, the 3-omega (3ω) method (Cahill, 1990) is used for measuring the thermal conductivity of nanofluids. The micro-electro-mechanical systems (MEMS) fabrication technique is used to fabricate a 3ω device. Using the microfabricated 3ω device,

* Corresponding author. Tel.: +82 (2) 880 7117; fax: +82 (2) 883 0179.
E-mail address: jslee123@snu.ac.kr (J.S. Lee).

0142-727X/$ - see front matter
doi:10.1016/j.ijheatfluidflow.2008.04.007

Nomenclature

b	half width of heater line (m)
C_p	substrate specific heat (J/kg K)
D	particle diameter (m)
g	gravitational acceleration (m/s^2)
I	current (A)
i	imaginary number
k	thermal conductivity (W/m K)
$\dot{Q}'$	heat flux (W/m)
q	complex thermal wave number
R	resistance (Ω)
T	temperature (K)
u	sedimentation velocity of nanoparticle (m/s)
V	voltage (V)
Greek symbols	
ΔT	temperature oscillation (K)
κ	integration variable
μ	viscosity of fluid (Pa s)
ρ	density of semi-infinite substrate (kg/m^3)
ω	angular frequency (rad/s)
Subscript	
f	property of the base fluid
h	temperature amplitude of the heater
i	imaginary part
nf	property of the nanofluid
r	real part
s	property of the solid particle
sub	property of the substrate

the thermal conductivity of the nanofluid can accurately be measured with a single droplet of sample fluid volume. Another advantage of the present method is that the gravitational effect on the nanofluid thermal conductivity can be examined by simply changing the orientation of the 3ω device. Additionally, the colloidal stability of the nanoparticle suspension can be evaluated in an easier way by detecting the thermal conductivity increment caused by nanoparticle sedimentation in a wider nanoparticle volume fraction range compared to the indirect methods such as measurement of surface charge of the particle (Lee et al., 2006) or detection of small angle X-ray scattering (Chen et al., 2008). In the present study, the thermal conductivities of Al_2O_3 nanofluids in de-ionized (DI) water or EG are measured by the 3ω method for different concentrations of nanoparticle, varying from 1% to 4% in Al_2O_3 volume fraction.

2. 3ω Method and thermal modeling

The 3ω method is widely used to measure the thermophysical properties of thin films and solid substrates (Jacquot et al., 2002; Jain and Goodson, in press). A sinusoidal electric current with an angular frequency of ω is passed through a thin film metal heater patterned on the solid substrate of interest. The metal heater also acts as a thermometer. Due to the sinusoidal heating at a double the frequency of the input current, the metal temperature also oscillates at an angular frequency of 2ω. Since the electrical resistance of the metal heater is a linear function of temperature, the temperature oscillation can be measured indirectly by measuring the associated 3ω voltage across the metal heater. The amplitude and phase of the temperature oscillation can be used to determine the thermophysical properties of the substrate since these parameters are related to each other through the solution of the energy equation for the given geometry and set of boundary conditions.

Consider a metal heater with width of 2b on a thick solid substrate. The relationship between the temperature oscillation and the heat generation rate can be expressed as (Cahill, 1990)

$$\Delta T = \frac{\dot{Q}'}{\pi k}\int_0^\infty \frac{\sin^2(\kappa b)}{(\kappa b)^2(\kappa^2+q^2)^{1/2}}\,d\kappa = \frac{\dot{Q}'}{\pi k}F(qb) \tag{1}$$

$$q = \sqrt{\frac{i2\omega\rho C_p}{k}} \tag{2}$$

$$\Delta T = \Delta T_r + i\Delta T_i \tag{3}$$

where ΔT represents the complex 2ω temperature oscillation, $\dot{Q}'$ the heating power per unit length generated at the metal heater, k the thermal conductivity of the substrate, q the complex thermal wave number, ω the angular frequency of the input current, and ρ and C_p are the substrate density and heat capacity, respectively. ΔT can further be decomposed into the real part or "in phase" term (ΔT_r) and the imaginary part or "out-of-phase" term (ΔT_i). The magnitude of ΔT is the amplitude of the temperature oscillation and the argument is the phase lag between the temperature oscillation of the heater and the heating pulse. The amplitude of reciprocal of q, $|1/q|$, is known as the thermal penetration depth. By simply substituting the infinite integral part of Eq. (1) with a function $F(qb)$, the thermal resistance of the substrate can be expressed as $F(qb)/\pi k$. The thickness of the substrate must be much larger than the thermal penetration depth in order for Eqs. (1)–(3) to be valid.

In this work, the original method is extended for use in the case of heat transfer in parallel through two semi-infinite media. The nanofluid of interest is placed on a quartz substrate on which a thin metal heater is attached as shown in Fig. 1. The thermal modeling of the 3ω device and nanofluid system is conducted based on the modified boundary mismatch assumption proposed by Chen et al. (2004). The nanofluid on the quartz substrate is modeled as a thermal resistance from the heater to the ambient, as depicted in the thermal resistance circuit in Fig. 1. The total heat generated from the heater ($\dot{Q}'_{total}$) passes through either the nanofluid layer

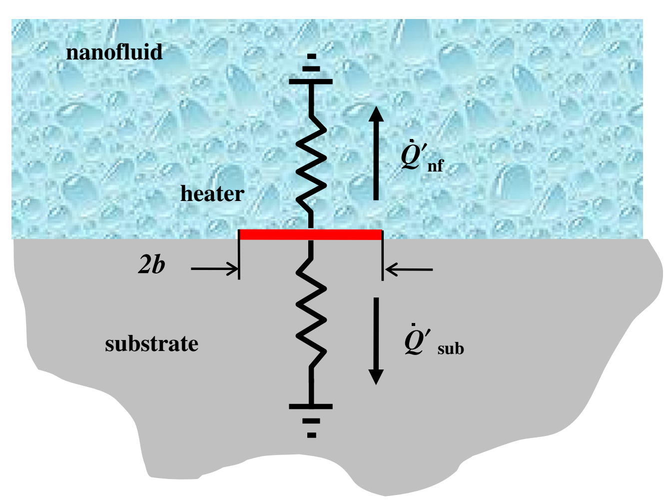

Fig. 1. Schematic and equivalent thermal circuit of the heater and two semi-infinite mediums of the nanofluid and the substrate.

($\dot{Q}'_{nf}$) or the substrate ($\dot{Q}'_{sub}$). The resistance at the fluid/substrate interface is neglected. This is a reasonable assumption when the thermal diffusivities of the fluid and the substrate are of similar values. Denoting the measured temperature oscillation of the heater in the presence of the nanofluid by ΔT_h, it can easily be shown that

$$\dot{Q}'_{total} = \dot{Q}'_{sub} + \dot{Q}'_{nf} = \frac{\Delta T_h}{\frac{F(q_{sub}b)}{\pi k_{sub}}} + \frac{\Delta T_h}{\frac{F(q_{nf}b)}{\pi k_{nf}}} \quad (4)$$

From the relationship between the temperature oscillation and the heat generation per unit heater length, given by Eq. (1), the heat flux term on right hand side of Eq. (4) can be replaced with the temperature oscillation per unit thermal resistance of the substrate and nanofluid layers, respectively. q_{sub}, q_{nf} and k_{sub}, k_{nf} denote the complex thermal wave number and thermal conductivity for the substrate and nanofluid layers, respectively. Multiplying Eq. (4) by $1/\Delta T_h$, a simple relationship between the temperature oscillations can be obtained as follows:

$$\frac{1}{\Delta T_h} = \frac{1}{\Delta T_{sub}} + \frac{1}{\Delta T_{nf}} \quad (5)$$

Note that ΔT_h is the measured temperature oscillation of the heater, with the substrate on one side and the nanofluid layer on the other. ΔT_{sub} is the heater temperature oscillation due to the heat transfer in the quartz substrate alone. In other words, ΔT_{sub} is measured in vacuum. A least squares fit of ΔT_{nf} calculated from Eq. (1) can be used to determine the value of the nanofluid thermal conductivity k_{nf}. The fitting frequency range is carefully selected to improve the accuracy of the fluid thermal conductivity calculation. In our case, the range of 4–250 Hz is found to provide the best results.

Since the substrate and the nanofluid layer are modeled as two separate semi-infinite media, their thicknesses must be chosen carefully. The thermal penetration depths in the substrate and the nanofluid at the lowest input frequency used in this work are 128 μm and 54 μm, respectively. In order to eliminate the substrate bottom boundary effect and to ensure validity of the semi-infinite assumption, 2 mm thick fused quartz wafer is used as a substrate. The nanofluid droplet size is controlled to be larger than 2 mm.

3. Sensor fabrication and validation of the 3ω device

The 3ω device was microfabricated at the Stanford nanofabrication facility (SNF) by metal deposition and patterning on a 2 mm thick fused quartz wafer. Twenty nanometre chromium and 200 nm platinum are sputtered and patterned by the liftoff method followed by PECVD deposition of a 400 nm SiO_2 passivation layer. The wet oxide etching is used to provide access to the contact pads. The wafer is then diced into individual devices, each of which is packaged in a ceramic chip carrier. Wire bonding facilitates electrical access to metal heaters. A 2.5 mm thick PDMS gasket is used to seal the device and to create a well in a 4×3 mm^2 region around the heater. Approximately 30 μl of nanofluid is placed inside the PDMS well. A schematic of the 3ω device cross-section and the top view is depicted in Fig. 2. Besides containing the nanofluid layer, the PDMS gasket also helps prevent any damage to wire bonds during device usage.

The microdevice is placed inside a temperature controlled cryostat (Model 330, Lakeshore) and all experiments are conducted at room temperature (21 °C). The metal heater in the microdevice is configured as part of a balanced Wheatstone bridge, and a lock-in amplifier (SR830, Stanford Research) is used to accurately measure the 3ω voltage across the metal heater. The temperature oscillation from the measured 3ω voltage ($V_{3\omega}$) is calculated as follows:

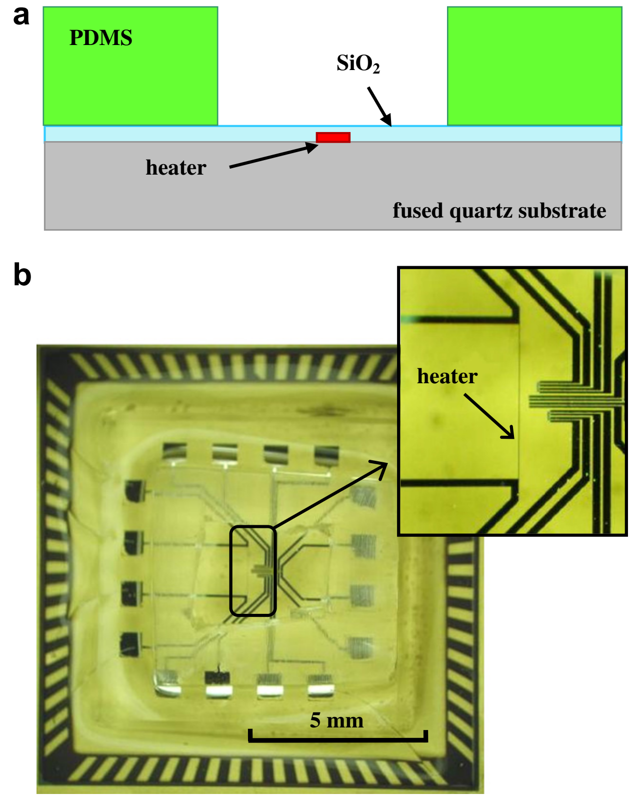

Fig. 2. Microfabricated heater device for measuring thermal conductivity of nanofluid: (a) cross-section of the heater on 2 mm thick quartz substrate (not to scale) and (b) top view of the 3ω device.

$$\Delta T_h = 2\frac{V_{3\omega}}{I_h}\frac{\partial T}{\partial R} \quad (6)$$

where I_h is the current at frequency ω across the microheater and $\partial T/\partial R$ is the ratio of temperature change with respect to the resistance change of the microheater. The temperature oscillation of the fused quartz substrate is first measured in vacuum, and the in-phase and out-of-phase temperature amplitudes as a function of current frequency are plotted in Fig. 3. The substrate thermal conductivity is calculated to be 1.3 W/m K which agrees well with the table value of bulk fused quartz (Çengel, 1998).

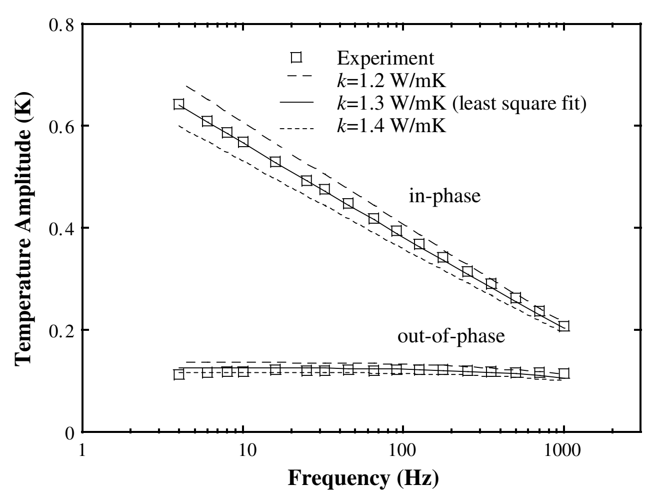

Fig. 3. Measured in-phase and out-of-phase temperature amplitude of fused quartz substrate in vacuum.

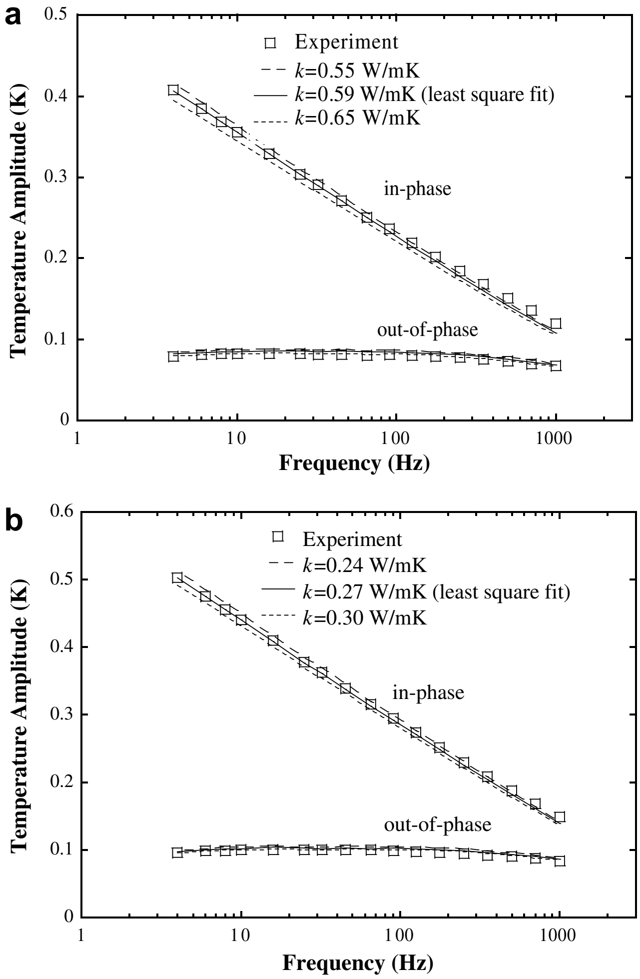

Fig. 4. Comparison of experimental temperature amplitudes with calculated value for: (a) DI water and (b) EG with various thermal conductivities.

The thermal model presented in the previous section is validated by comparing with the measured thermal conductivities from the 3ω response of DI water and EG. The amplitude of input current to the 3ω device is selected in such a way that the maximum temperature rise of the heater is always maintained at less than 0.5 K. The typical heat generation from the heater is 1.26 mW. Fig. 4a and b show the measured temperature oscillation of DI water and EG respectively. The least squares values of the measured thermal conductivity in comparison with the model are 0.591 ± 0.004 W/m K and 0.267 ± 0.003 W/m K for DI water and EG respectively, both of which are in good agreement with the standard values at room temperature of 0.60 W/m K and 0.26 W/m K (Çengel, 1998), respectively. The slight deviation may arise from experimental uncertainty and from the difference in the thermal diffusivity between the fluid and the fused quartz substrate, which may induce heat transfer between the fluid/substrate interface. The measurement uncertainty mainly comes from the uncertainty of the $V_{3\omega}$ (about 2%). The measured values of I_h and $\partial T/\partial R$ are very stable with less than 0.2% deviation. Thus, the uncertainty of the temperature oscillation can be estimated as about 2% from Eq. (6). After confirming the validity of the present model, the effective thermal conductivity of Al_2O_3 nanoparticles in DI water and EG is measured.

4. Nanofluid preparation and the gravity effect

The nanofluids are prepared by mechanically mixing the commercial Al_2O_3 nanoparticle powder (aluminum oxide, NanoTek®) with the base fluid. The Al_2O_3 nanoparticles are generally spherical in shape, with an average particle size of 45 nm. To ensure homogeneous dispersion, the mixture of the base fluid and nanoparticles is ultrasonically vibrated for over 15 h in an ultrasonic cleaner (FS60, Fisher Scientific). No visual sedimentation is observed after the ultrasonic vibration step. Furthermore, the nanoparticles are not observed to adhere to the 3ω device during the experimental period. However, the nanofluid samples exhibit a continuous decrease in the amplitude of 2ω temperature oscillation with time at each current frequency. This phenomenon is illustrated in Fig. 5, where the 2ω temperature amplitude of 1% volume fraction of the DI water nanofluid is measured at the fixed current frequency of 125 Hz as a function of time. The reason for the continuous decrease in the temperature amplitude is believed to be the gradual thermal conductivity rise of the nanofluid sample.

In order to investigate the presumed effect of the gravitational field in this observation, the sedimentation velocity is estimated based on the force balance between the buoyancy force and the Stokes drag force exerted on a 45 nm diameter Al_2O_3 sphere immersed in water. The sedimentation velocity u can be expressed as

$$u = \frac{(\rho_s - \rho_f)g}{18\mu} D^2 \tag{7}$$

where ρ_s and ρ_f are the densities of the particle and the fluid, respectively. g is the gravitational acceleration, μ is the viscosity of the fluid, and D is the particle diameter. The settling velocity of the nanoparticle obtained from Eq. (6) is 3.1 nm/s. During the experimental period of 10 min, a single nanoparticle travels only 2 μm due to the sedimentation. This distance is negligible compared to the droplet size. This back-of-the-envelope calculation suggests that the gravitational effect may be negligible. However, an additional experimental investigation provides evidence that the gravity effect on the nanofluid may indeed be responsible for the observed continuous decrease in the temperature amplitude with time.

The nanofluid thermal conductivity is measured at different microheater orientations with respect to the gravitational field. The nanofluid droplet placed on the test device is small enough to have negligible shape change when it is turned upside down. Fig. 5 shows data measured at different orientations to the gravitational field. It is observed that when the nanofluid is heated from the top, the temperature amplitude first increases during the first

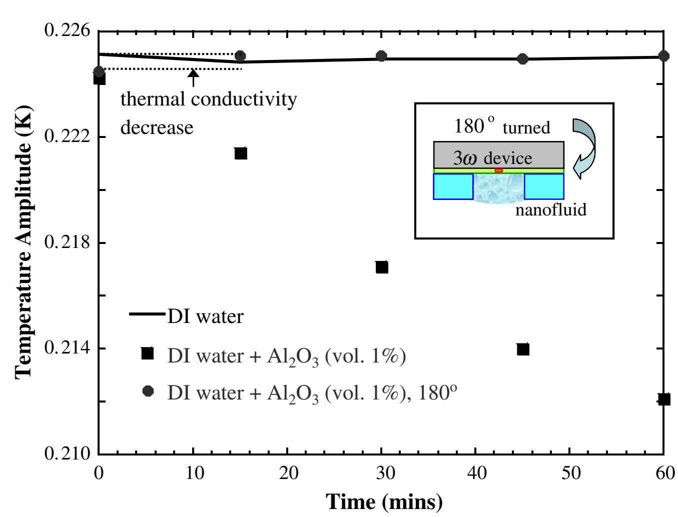

Fig. 5. Temperature amplitude changes of nanofluid at upright and upside down (180° turned) heater positions with respect to time at 125 Hz of input current frequency.

15 min and then converges to the separately measured DI water temperature amplitude. This indicates that gravity causes a decrease in the nanoparticle concentration within the thermal penetration depth. Clearly, this contradicts the analysis presented above.

Gravitation causes natural convection or particle sedimentation within the nanofluid droplet. It is easy to estimate the natural convection effect within the nanofluid droplet on the sensor since the maximum temperature rise of the heater is always maintained less than 0.5 K. The configuration of the nanofluid can be simplified as a horizontal layer, where the bottom surface is heated and the top surface is cooled. The Rayleigh number determines the strength of natural convection effect. For the Rayleigh number less than the critical value of 1708, it is well known that the fluid inside the horizontal layer is stagnant, and the Nusselt number is unity (Hollands et al., 1975). In such a case, only conduction heat transfer occurs across the horizontal layer and thus natural convection can be ignored. Since the present Rayleigh number is around 250, the natural convection effect is surely negligible. One possible source is that the nanoparticles may not have been completely deagglomerated by the ultrasonic agitation.

To rule out the gravity effect on 3ω measurements of DI water based nanofluids, the maximum temperature amplitude values obtained from two separate experiments in the directions of increasing frequency and of decreasing one are compared at each frequency point. Fig. 6 shows the temperature amplitude as a function of the current frequency for the DI water based nanofluid of 4% volume fraction. The thermal conductivity of the 4% volume fraction DI water based nanofluid is considered to be most influenced by gravity, among the rest of nanofluid samples used in this work. The data for the DI water based nanofluid at two different frequency directions show slight deviation in Fig. 6. While on the other, for the EG nanofluid the data coincide exactly with each other and thus they are not plotted here. This implies that the sedimentation of agglomerate nanoparticles is negligible in a denser and more viscous fluid like EG compared to the DI water.

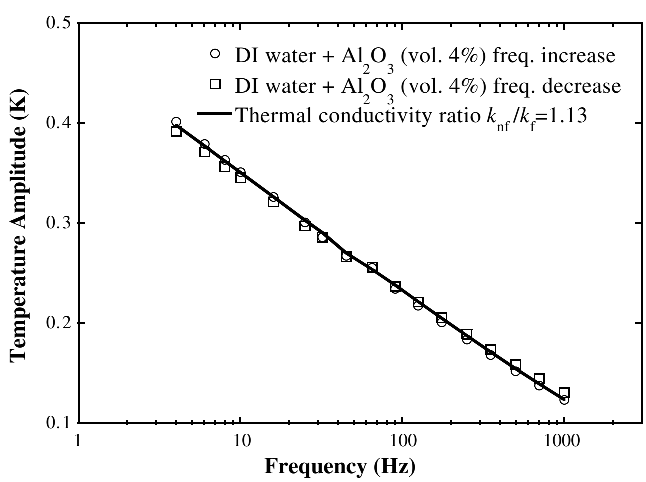

Fig. 6. Temperature amplitude variations of increasing and decreasing input voltage frequency for DI water nanofluid (vol. 4%).

By the least squares fit of the theoretical model, a 4% volume fraction Al_2O_3 nanofluid in the DI water shows 13.3% increase in the thermal conductivity compared to the base fluid. If the thermal conductivity of the nanofluid is fitted with all data points averaged, a 15.5% increase is observed. The difference of 2.2% in the thermal conductivity enhancement may be due to agglomeration and sedimentation of nanoparticles. In analyzing EG based nanofluids, temperature amplitude data at a single frequency is averaged.

5. Experimental results and discussion

The measured thermal conductivity values for DI water and EG nanofluids are presented in Table 1a and b, respectively. The thermal conductivity of the nanofluids shows monotonously increasing behavior with the nanoparticle volume fraction. Our data shown in the table fall in the tolerable range compared to other data measured at room temperature. For the DI water based nanofluids, the thermal conductivity increment data agrees well with those of Wang et al. (1999), which show higher increment in comparison with the results of Lee et al. (1999) and Das et al. (2003). On the other hand, the present EG based nanofluids data shows relatively low thermal conductivity values compared to those of Lee et al. (1999) and Wang et al. (1999).

At this moment it cannot be clearly explained the reason why the discrepancy takes place among the measurements of the nanofluid thermal conductivity because of various sources of measurement uncertainties such as sedimentation and aggregation of nanoparticles, nanofluids preparation, and so forth. The nanoparticles used in the above referred experiments and those used in the present research are believed to be the same product by Nanophase Technologies Corp., (Burr Ridge, IL), although the particle diameter mentioned in each paper differs because of different particle size analysis methods being used. Wang et al. (1999) seem to

Table 1
Measured enhancement of thermal conductivity ratios of nanofluids (a) DI water nanofluids, (b) EG nanofluids

Al_2O_3 nanoparticle volume fraction (%)	Present experiment	Lee et al. (1999)	Wang et al. (1999)	Das et al. (2003)
(*a*) *DI water nanofluids*				
0	1.000 ± 0.006	–	–	–
1	1.044 ± 0.002	1.03	–	1.02
2	1.077 ± 0.005	1.05	–	1.05
3	1.112 ± 0.010	1.07	1.11	1.07
4	1.133 ± 0.008	1.09	–	1.09
4.3	–	1.10	–	–
4.5	–	–	1.15	–
5.5	–	–	1.15	–

Al_2O_3 nanoparticle volume fraction (%)	Present experiment	Lee et al. (1999)	Wang et al. (1999)
(*b*) *EG nanofluids*			
0	1.000 ± 0.013	–	–
1	1.019 ± 0.007	1.03	–
2	1.027 ± 0.010	1.06	–
3	1.075 ± 0.004	1.10	–
4	1.097 ± 0.004	1.14	–
5	–	1.18	1.25
8	–	–	1.41

use either a mechanical blending method or a filtration method in the nanofluid preparation process where the particles larger than 1 μm in diameter are removed from the suspension. Although the filtration may cause uncertainty in the evaluation of the nanoparticle volume fraction, the large aggregated nanoparticles that could still exist even after severe ultrasonic vibration can be filtered out. Das et al. (2003) applied ultrasonic vibration to nanofluids for 12 h which is comparable to ours of 15 h. Since our nanofluids show clear sign of sedimentation within a few minutes after they are taken out of the ultrasonic cleaner, the gravity effect may also be present in Das et al.'s data. The details of the preparation method are not described other than "shaken thoroughly" in the paper of Lee et al. (1999).

In comparing the thermal conductivity measurement techniques, the steady state parallel plate method used by Wang et al. (1999) seems to be least affected by the particle sedimentation for their thickness of the loaded sample fluid is less than 1 mm. On the other hand, the transient hot wire method used by Lee et al. (1999) can be affected by the sedimentation of nanofluids. Non-homogeneous nanoparticle concentration in the direction of gravity can give rise to temperature gradient within the vertical hot wire, which may be a source of measurement errors. This is also true for the temperature oscillation technique by Das et al. (2003) where the thermocouple that measures the fluid temperature oscillation lies in the upper half of the nanofluid chamber. The time duration between the nanofluids preparation and the measurement, and the measuring time are also important factors since the particle aggregates tend to grow with time, but it cannot be compared for lack of sufficient information in the literature. Further study is required to reduce the sedimentation of nanofluids by adding an appropriate chemical additive or by utilizing the mechanical method such as filtering or centrifuge of nanoparticle aggregates to reduce the experimental uncertainties.

6. Conclusion

This paper reports experimental data of the thermal conductivity enhancement in Al_2O_3 nanofluids with DI water and EG as base fluids by using the modified 3ω method. Cahill's heat transfer model for the 3ω method (1990) is extended in two parallel semi-infinite media. The present model is validated by thermal conductivity measurements of pure DI water and EG, which agree well with the standard values.

The thermal conductivity of the nanofluid is observed to continuously increase with time. Gravitational effect on the nanoparticle aggregates is believed to be the reason behind this observation. Increase in thermal conductivity due to sedimentation effect is also measured quantitatively. Filtering of the experimental data has been performed in order to exclude the gravitational effect on the measured nanofluid thermal conductivity.

Compared with the conventional thermal conductivity measurement methods, the proposed 3ω measurement technique offers several advantages. The 3ω method can be used to determine whether homogeneous mixing is achieved for the stationary nanofluid with only a small sample volume. In addition, the measurement of the spatial variation of the thermal conductivity is possible which may provide insight into the thermophysics of the aggregation process. The 3ω method proposed in this work can easily be extended to investigate the temperature or pressure dependence on the nanofluid thermal conductivity.

Acknowledgements

This work is supported by the Micro Thermal System Research Center, Seoul National University. Use of facilities at the Stanford Nanofabrication Facility (SNF) is gratefully acknowledged.

References

Cahill, D.G., 1990. Thermal conductivity measurement from 30 to 700 K: the 3ω method. Rev. Sci. Instrum. 61, 802–808.

Çengel, Y.A., 1998. Heat Transfer: A Practical Approach. McGraw-Hill, NJ.

Chen, F., Shulman, J., Xue, Y., Chu, C.W., Nolas, G.S., 2004. Thermal conductivity measurement under hydrostatic pressure using the 3ω method. Rev. Sci. Instrum. 75, 4578–4584.

Chen, G., Yu, W., Singh, D., Cookson, D., Routbort, J., 2008. Application of SAXS to the study of particle-size-dependent thermal conductivity in silica nanofluids. J. Nanopart. Res. doi: 10.1007/s11051-007-9347-y.

Das, S.K., Putra, N., Thiesen, P., Roetzel, W., 2003. Temperature dependence of thermal conductivity enhancement for nanofluids. J. Heat Transfer 125, 567–574.

Hamilton, R.L., Crosser, O.K., 1962. Thermal conductivity of heterogeneous two-component systems. I & EC Fundamentals 1, 182–191.

Hollands, K.G.T., Raithby, G.D., Konicek, L., 1975. Correlation equations for free convection heat transfer in horizontal layers of air and water. Int. J. Heat Mass Transfer 18, 879–884.

Hong, K.S., Hong, T.K., Yang, H.S., 2006. Thermal conductivity of Fe nanofluids depending on the cluster size of nanoparticles. Appl. Phys. Lett. 88, 031901.

Jacquot, A., Lenoir, B., Dausher, A., Stölzer, M., Meusel, J., 2002. Numerical simulation of the 3ω method for measuring the thermal conductivity. J. Appl. Phys. 91, 4733–4738.

Jain A., Goodson, K.E., in press. Measurement of the thermal conductivity and heat capacity of free-standing shape memory thin films using the 3-ω method. J. Heat Transfer.

Kabelac, S., Kuhnke, J., 2006. Heat transfer mechanisms in nanofluids – experiments and theory. In: Proceedings of the 13th IHTC, 13–18 August, 2006, Sydney, Australia.

Lee, S., Choi, S.U.S., Li, S., Eastman, J.A., 1999. Measuring thermal conductivity of fluids containing oxide nanoparticles. J. Heat Transfer 121, 280–289.

Lee, D., Kim, J.W., Kim, B.G., 2006. A new parameter to control heat transport in nanofluids: surface charge state of the particle in suspension. J. Phys. Chem. B. 110, 4323–4328.

Marquis, F.D.S., Chibante, L.P.F., 2005. Improving the heat transfer of nanofluids and nanolubricants with carbon nanotubes. JOM 57, 32–43.

Masuda, H., Ebata, A., Teramae, K., Hishinuma, N., 1993. Alteration of thermal conductivity and viscosity of liquid by dispersing ultra-fine particles (dispersion of γ-Al_2O_3, SiO_2 and TiO_2 ultra-fine particles). Netsu Bussei (Japan) 4, 227–233.

Maxwell, J.C., 1892. A Treatise on Electricity and Magnetism. Oxford University Press, London.

Prasher, R.S., Bhattacharya, P., Phelan, P.E., 2006. Effect of aggregation kinetics on the thermal conductivity of nanoscale colloidal solutions (nanofluid). Nano Lett. 6, 1529–1534.

Wang, X.Q., Mujumdar, A.S., 2007. Heat transfer characteristics of nanofluids: a review. Int. J. Therm. Sci. 46, 1–19.

Wang, X., Xu, X., Choi, S.U.S., 1999. Thermal conductivity of nanoparticle-fluid mixture. J. Thermophys. Heat Transfer 13, 474–480.